

Memory-Integral Mass-Transfer Models for Adsorption Process Simulation

George M. Harriott

Air Products and Chemicals, Inc., Allentown, PA 18195

The memory integral based on convolution of the unit step response to loading a clean pellet with concentration history at the pellet surface is proposed for computations of mass transfer in adsorption process simulation. Although rate laws are widely used to describe diffusion and sorption in pellets for slow (Glueckauf, 1955) and moderate (Kim, 1989) rates of mass transfer, these models fail to describe mass transfer at short contact times because the concentration history experienced by the pellet is not accounted for. To facilitate memory integral computations, approximations to the unit step response to loading a clean pellet are derived based on a single moving finite element and by asymptotic matching in time. Numerical evaluation of the memory integral is demonstrated on simple cycles which show the merits of this approach.

Introduction

The diffusion rate of gases in and out of pelletized solids is a significant factor in many chemical processes, particularly in adsorption. When gases are separated by equilibrium with a solid, the rate of transport to the active surface of the adsorbent will limit the purity of the product stream. Accordingly, equilibrium separations are designed to operate over a period that is large compared to the characteristic diffusion time. On the other hand, kinetic separations rely on the diffusion timescale for one species being long relative to the process time. To be useful for simulation then, a general model for sorption dynamics must accurately represent diffusion over a wide range of timescales.

Adsorption processes are typically carried out in "beds" consisting of large columns packed with a multitude of small pellets to promote contact between fluid and solid. Species in the feed stream are fractionated by the solid on an "adsorption" step which is then followed by a sequence of "rinse" or "purge" steps to clean out the solid so that it may be used again. The dynamics vary in detail throughout the column, but at each point eventually a cyclic or periodic state is reached in which the particles undergo equal amounts of adsorption and desorption.

In models of adsorption processes, mass transfer within the pellets is set fundamentally by a diffusion equation, and the dynamics of all pellets are linked by boundary conditions at the external surfaces swept by the flowing stream. Flow is directed along the column axis so that the collective behavior

of the system is essentially one-dimensional. A differential mass balance on an intermediate lengthscale that is large compared to a single pellet, but small in relation to the column dimensions requires that:

$$\epsilon \frac{\partial \Gamma}{\partial t} + \frac{\partial (v\Gamma)}{\partial z} + (1 - \epsilon) \frac{\partial L}{\partial t} = 0, \quad (0)$$

where Γ is the concentration in the flowing stream, L is the loading in the immobile solid, v is the superficial velocity, and ϵ is the void fraction between pellets. Here z measures distance along the column axis and t represents time. Energy and momentum balances are required to complete the set of column equations if the process is not isothermal or if pressure gradients are significant.

The hyperbolic nature of the mass balance, Eq. 0, supports waves (Aris and Amundson, 1973) which wash conditions imposed from an inlet through the column. Equilibrium, which acts either to sharpen or smear the wavefront, controls the dynamics when the wavespeed is slow. In idealized circumstances, spreading of the front by mass transfer is exactly balanced by equilibrium sharpening, and a "constant-pattern" wave forms which effects a transition from uniform conditions ahead of the wave to fixed boundary conditions behind (Gorius et al., 1991). At the other extreme, waves pass through the column quickly and establish a uniform concentration in the

external fluid to which the pellets then equilibrate. This is the case of "batch sorption" by the bed. These simple cases are characteristic of mass transfer in process operation, though the dynamics at an arbitrary point in a column is often abstruse and not plainly linked to boundary conditions.

In the general case, adsorption process dynamics are determined numerically by temporal integration of spatially discretized forms of Eq. 0 and other governing partial differential equations. Stability considerations favor *implicit* integration in time and the computational labor, though reasonable for one-dimensional column equations, grows sharply with additional spatial dimensions. Numerical solution of the diffusion equation within the pellets coupled with implicit process simulation is therefore a computationally intensive task. For this reason, diffusion transport models, which predict the mass-transfer rate as a function of loading in the pellet and concentration in the external fluid are widely used for process design.

For equipment design or highly refined process simulation, multidimensional calculations are required. Calculations of fluid maldistribution in adsorption columns for example could involve three macroscopic dimensions plus the pellet radius for a total of four spatial dimensions! Partially *explicit* integration schemes like those used in transient fluid dynamic simulation (Oran and Boris, 1987) are likely to be favored for multidimensional adsorber simulations of this sort, because the computational work grows linearly with the number of unknowns. With explicit integration, there may be little extra cost in coupling the numerical solution of the diffusion equation with the column dynamics. These are very large-scale calculations, however, and are not likely to supplant simpler models used for generic process design.

The fundamental features of diffusional mass transfer within pellets are displayed clearly by the *unit step response*, initiated by subjecting a saturated (typically clean) pellet to an abrupt change of unit magnitude in external concentration. Pellets respond to a jump in external concentration with infinite flux, and then slow down and approach saturation monotonically. Mass transfer at short times is driven by the difference between initial and boundary conditions, whereas at long times the flux is proportional to the departure from saturation. From the unit step response, the general solution to the linear diffusion equation is constructed by convolution with the variation of external concentration (Carslaw and Jaeger, 1959), but due to its perceived complexity this exact formula is rarely exercised in process simulation.

The most widely used approximate rate model, known as the Linear Driving-Force law (LDF), was also the earliest one. It was proposed by Glueckauf and Coates (1947) for the transient response of the loading L in a pellet of radius R to changes in external concentration as:

$$\frac{dL}{dt} = K \left[\frac{D_e}{R^2} \right] (E - L), \quad (1)$$

in which K is a dimensionless mass-transfer coefficient, D_e is an effective diffusivity, and E is the loading in equilibrium with the external fluid. The value of $K = 15$ has been adopted for this model based on comparison with experimental data and approximate analysis of the diffusion equation.

Formal justification of the LDF rate law is based on asymptotic expansion at long times of the general solution to the

diffusion equation. The leading term of the approximation is of the LDF form, with a coefficient of $K = 15$ (Glueckauf, 1955). Frequency analysis of the diffusion equation (Jury, 1967) confirms these results at slow modulation. Recently, Kim (1989) has extended the formal derivation to obtain a mass-transfer law based on second-order truncation, which extends the region of validity to moderate rates of mass transfer.

Most published derivations of the LDF rate equation for sorption do not start with the exact solution, but rather have *assumed* the form of the spatial concentration profile in the pellet. The diffusion equation is then integrated across the pellet and a relation obtained between the rate of uptake and the mean concentration in the pellet at any time. Liaw et al. (1979) showed that the standard value of $K = 15$ could be derived with a parabolic profile. With this method, additional physics may be accommodated; for example, Doong and Yang (1987) assumed parabolic profiles to derive a rate equation that incorporated the different resistances of macropores and micropores in the pellet.

Comparison with the exact solution of the unit step response, however, shows that the rate law derived with a parabolic profile severely underpredicts the rate of sorption at short contact times (Do and Rice, 1986). Modifications to the assumed concentration profile to compensate for this error have included quartic terms (Do and Rice, 1986) and higher-order even powers in pellet radius (Tomida and McCoy, 1987). Cubic terms in radius were considered by Buzanowski and Yang (1989), and a power-law exponent, which is a function of time, was proposed by Do and Mayfield (1987). All of these analyses result in a better fit to the standard problem of uptake into a clean pellet, though none fully capture the singular behavior of the unit step solution at small times.

When E is constant, as for example with "irreversible" adsorption, Vermeulen (1953) claimed that a quadratic difference from equilibrium resulted in a superior fit to the rate of saturation:

$$\frac{dL}{dt} = K \left[\frac{D_e}{R^2} \right] \frac{(E^2 - L^2)}{2L}, \quad (2)$$

in which the value of the mass-transfer coefficient was set to $K = \pi^2$. Equation 2 is the Quadratic Driving-Force (QDF) law. Note that Eq. 2 is linear in loading squared and singular as $L \rightarrow 0$. When the equilibrium was strongly nonlinear, Glueckauf (1955) observed that the leading edge of the constant-pattern wave is sharp and recommended the QDF formula on this basis. For particles of intermediate adsorption affinity, a modified quadratic formula was recommended, but the connection to the diffusion equation was not made clear.

Despite the improved fit to the classic uptake problem, these mass-transfer models have not been used in process simulation, chiefly because the resulting expressions do not properly generalize to the complex concentration history set by Eq. 0 throughout an adsorption bed. Models offering improved accuracy for adsorption at short times tend to represent desorption poorly, notwithstanding that in a cyclic process both steps are of comparable importance. Typically, the LDF model continues to be used, and the deficiency at short times is corrected by increasing the mass-transfer coefficient from the standard value of 15, according to the ratio of process and diffusion

timescales (Nakao and Suzuki, 1983; Raghavan et al., 1986). Such modification to the LDF law accounts for the gross effects of short cycle times, but does not make for accurate simulation.

An alternate computation of mass transfer in adsorption processes is based directly on the integral form of the general solution to the diffusion equation. This approach was used in the classical analysis of the saturation wave in a linear system (Rosen, 1952), in studies of cyclic process performance under nonlinear equilibrium (Bunke and Gelbin, 1975, 1978) and has been applied to fit batch sorption data (Kocirik et al., 1988). The results presented in all these articles were at long contact times on the scale of the pellet however, and so could have been predicted by rate equations such as the LDF model. No comparison was made with differential models of mass transfer, and the accuracy of the integral formulation at short contact times was not emphasized.

In view of the limited ability of differential rate models to capture both short and long timescales in a manner suitable for process simulation, it is appropriate to give the integral formulation due consideration. For effective use in process simulation, however, it will be necessary to evaluate the convolution integral quickly, and as part of this effort, develop a succinct approximation of the unit step response. The first steps toward this goal are presented in this article. Equations governing diffusion and sorption in the pellet are reviewed with the general solution and the limit at long times. Recognizing the distinct features of the early and late time character of the unit step response permits accurate approximations to be developed. Because significant contributions to convolution fall within the saturation timescale or "diffusional memory" of the pellet, the integral is a *memory integral* and may be computed efficiently. Finally, predictions based on rate laws are compared with memory integral solutions for two simple cycles.

Theory

The approximations developed here are based on diffusion and adsorption of a single component in a spherical pellet. Both adsorbed and gaseous phases may be considered to diffuse, so the mass balance equation is:

$$\frac{\partial N}{\partial t} = \frac{1}{x^2} \frac{\partial}{\partial x} \left(x^2 \left[D_c \frac{\partial C}{\partial x} + D_s \frac{\partial S}{\partial x} \right] \right), \quad (3)$$

in which x is the radial coordinate and t represents time. C and S are the interstitial gas and adsorbed concentration within the pellet and N is the total concentration: $N = \nu C + (1 - \nu)S$, with ν being the void fraction of internal pore space. Here the adsorbed material is assumed to be locally at equilibrium with the mobile species in the interstitial gas.

To cast the problem in dimensionless form, vapor concentration is scaled with a peak value C^* , and adsorbed concentration with the corresponding equilibrium loading S^* so that the total concentration at any point in the pellet is scaled as $N^* = \nu C^* + (1 - \nu)S^*$. Distances are made dimensionless with the pellet radius R , and the timescale is $t^* = R^2/D_c$ where the effective diffusivity is defined as $D_e = [C^*D_c + S^*D_s]/N^*$. To keep notation uncluttered, dimensionless variables will be denoted with the same symbols as their physical counterparts (dimensionless variables are simply physical variables meas-

ured by their respective scales). The mass-balance equation then reads:

$$\frac{\partial N}{\partial t} = \frac{1}{x^2} \frac{\partial}{\partial x} \left(x^2 D(C) \frac{\partial C}{\partial x} \right), \quad (4)$$

where the diffusion function is defined as $D(C) = [C^*D_c + S^*D_s f(C)]/[C^*D_c + S^*D_s]$, and $f(C)$ is the local slope of the dimensionless isotherm. Note that $D(C) = 1$ if surface diffusion is absent or the isotherm is linear.

The usual approach in deriving approximate solutions to Eq. 4 starts with the problem of linear equilibrium in which $S = C$, and then generalizes the linear result to a nonlinear adsorption relationship by substitution of $S = E(C)$. Errors introduced by this procedure are discussed briefly at the conclusion of this article. The dimensionless problem is thus reduced to the standard diffusion equation in the pellet ($0 \leq x \leq 1$) for which $N = C$:

$$\frac{\partial C}{\partial t} = \frac{1}{x^2} \frac{\partial}{\partial x} \left(x^2 \frac{\partial C}{\partial x} \right), \quad (5)$$

with boundary conditions of:

$$C(1, t) = \Gamma(t), \quad (6a)$$

$$\frac{\partial C(0, t)}{\partial x} = 0, \quad (6b)$$

and initial condition of $C(x, 0) = C_0(x)$. External resistance to mass transfer is typically small and has been neglected to show clearly the dynamics of the pellet itself. Process dynamics, described by Eq. 0, depend on the pellet loading which is obtained by integrating the total concentration:

$$L(t) = 3 \int_0^1 C(x, t) x^2 dx. \quad (7)$$

Because the model is linear, the solution may be constructed by convolution of the unit step response with the variation of external concentration (Carslaw and Jaeger, 1959):

$$C(x, t) = \int_0^t \frac{\partial \Gamma}{\partial t}(s) F(x, t-s) ds, \quad (8a)$$

$$L(t) = \int_0^t \frac{\partial \Gamma}{\partial t}(s) \Psi(t-s) ds, \quad (8b)$$

where F and Ψ represent the unit step responses to the diffusion equation for concentration and loading, respectively.

The case of uptake by a clean pellet corresponds to the unit step response and is defined by $C_0(x) = 0$, $\Gamma(t) = 1$. This solution is readily derived by integral transforms and may be written as a Fourier series (Carslaw and Jaeger, 1959):

$$F(x, t) = 1 + 2 \sum_{n=1}^{\infty} \frac{\sin(n\pi x)}{n\pi x} (-1)^n e^{-(n\pi)^2 t}, \quad (9a)$$

$$\Psi(t) = 1 - 6 \sum_{n=1}^{\infty} \frac{1}{(n\pi)^2} e^{-(n\pi)^2 t}. \quad (9b)$$

Note that the eigenfunctions are $\sin(n\pi x)/n\pi x$. This is because the diffusion equation in spherical geometry may be transformed to the planar case by the variable C/x and has implications for the choice of spatial profile when constructing approximate solutions of the unit step response, as will be discussed later. The loading of the pellet approaches saturation exponentially slowly with rate of π^2 . At small times, the features of the solution are displayed more clearly by Laplace transformation which shows that initially the loading rises as $L(t) = 6\sqrt{t/\pi}$. The singularity in the mass-transfer rate arises from the initial discontinuity in concentration between the pellet and the external fluid and is the root cause of error in the LDF and like models at small contact times.

When the modulation of the surface concentration is slow on the timescale of pellet saturation, an asymptotic series approximation of the general solution may be derived by integrating Eq. 8a by parts. The terms of the resulting series may be summed exactly in Fourier space to reveal polynomial variation of concentration within the pellet:

$$C(x, t) = \Gamma(t) + (1-x^2) \left(\frac{1}{6} \frac{\partial \Gamma}{\partial t} + \frac{1}{36} \frac{\partial^2 \Gamma}{\partial t^2} + \dots \right) - (1-x^4) \left(\frac{1}{120} \frac{\partial^2 \Gamma}{\partial t^2} + \dots \right) + \dots \quad (10a)$$

Because rate derivatives scale with the ratio of timescales, the leading form of the spatial concentration profile is seen to be parabolic, as assumed in many approximate solutions. The loading is given explicitly as:

$$L(t) = \Gamma(t) - \frac{1}{15} \left(\frac{\partial \Gamma}{\partial t} - \frac{2}{21} \frac{\partial^2 \Gamma}{\partial t^2} + \dots \right). \quad (10b)$$

A general rate law may be derived by adding K -times the loading to the derivative of loading:

$$\frac{\partial L}{\partial t} = K(\Gamma - L) + \left(1 - \frac{K}{15} \right) \frac{\partial \Gamma}{\partial t} - \frac{1}{15} \left(1 - \frac{2K}{21} \right) \frac{\partial^2 \Gamma}{\partial t^2} + \dots, \quad (11)$$

which yields the standard LDF law with the choice $K = 15$ (Glueckauf, 1955) and a second-order truncation with $K = 21/2$ (Kim, 1989).

Approximate Solutions: Unit Step Response

To extend rate laws to short contact times, prevailing research has focused on improved approximations to saturation in a clean pellet. These derivations generally start with the assumption of simple spatial concentration profiles and integrate the diffusion equation over the pellet to generate a rate law for the dynamics of the loading $L(t)$. With this approach the history of surface concentration is not accounted for, and so these approximations are not generally useful. Accurate approximations of the unit step response can be used, however,

to simplify computation of the memory integral. In this section, these approximations will be reviewed, and new approximations will be developed which are uniformly accurate in time.

To develop approximate solutions of the diffusion equation we expand concentration in spatial basis functions, but truncate after the first term:

$$C(x, t) = 1 + A(t)\Phi(x) + \dots, \quad (12)$$

where the basis function $\Phi(x)$ is chosen for convenience and accuracy. This is similar in spirit to Fourier expansion which is used to express the exact solution. The amplitude $A(t)$ is set by integrating the mass balance, Eq. 5, over the pellet, weighted with $w(x)$:

$$\int_0^1 w(x) \frac{\partial C}{\partial t} x^2 dx = w(1) \frac{\partial C}{\partial x}(1, t) - \int_0^1 \frac{\partial C}{\partial x} \frac{dw}{dx} x^2 dx, \quad (13)$$

In deriving this equation, the spatial operator has been integrated by parts and the no flux condition at the center of the pellet has been accounted for.

If a uniform weight is chosen, the standard volume balance results:

$$\frac{1}{3} \frac{dL}{dt} = \frac{\partial C}{\partial x}(1, t), \quad (14)$$

which has the attraction of giving an equation for the dynamics of L directly. Physically this shows that the rate of uptake into the pellet is set by the flux at the surface.

Although Eq. 14 is exact, it cannot be solved without an independent relation between concentration gradient and loading. The necessary closure relation depends on the assumed spatial profile for $\Phi(x)$, and sets the accuracy of the solution. A better approximation may be had by Galerkin projection in which the equation is weighted with the basis function prior to integration. Galerkin projection forces the amplitude $A(t)$ to be orthogonal to the basis function (Strang and Fix, 1978) and is the method by which amplitudes of Fourier modes are determined in the exact solution.

The dynamic equation resulting from either volume balance or Galerkin projection with spatial profiles which span the pellet is the dimensionless form of the LDF law. For example, the unit step response is governed by:

$$\frac{dL}{dt} = K(1 - L), \quad (15)$$

which upon integration shows that the loading approaches saturation exponentially slowly with rate K . Table 1 compares the LDF coefficients derived with linear, $\Phi(x) = 1 - x$, and quadratic, $\Phi(x) = 1 - x^2$, profiles using both volume average

Table 1. Unit Step Response: LDF Coefficients

Method Basis	Volume Balance	Galerkin Projection
Linear	12.0	10.0
Quadratic	15.0	10.5

Table 2. Unit Step Response: Penetration Theory

Volume Balance: Linear Basis

$$Q = 4.50$$

$$t = \frac{(1-\delta)}{144} \{13 + \delta - 5\delta^2 - 9\delta^3\}$$

Volume Balance: Quadratic Basis

$$Q = 6.00$$

$$t = \frac{(1-\delta)^2}{720} \{29 + 22\delta + 9\delta^2\}$$

Galerkin Projection: Linear Basis

$$Q = 6.75$$

$$t = \frac{1}{10} \left\{ 6 - 9\delta + 3\delta^2 + \frac{15}{\sqrt{3}} \left[\tan^{-1} \left(\frac{1+2\delta}{\sqrt{3}} \right) - \frac{\pi}{6} \right] + \frac{1}{2} \ln \left[\frac{1+\delta+\delta^2}{3} \right] \right\}$$

Galerkin Projection: Quadratic Basis

$$Q = 5.00$$

$$t = \frac{2}{7} \left\{ 6 - 5\delta - \delta^2 - \frac{27}{2} \ln \left[\frac{9+2\delta-\delta^2}{10} \right] - \frac{35}{\sqrt{10}} \ln \left[\frac{1-\delta+\sqrt{10}}{\delta-1+\sqrt{10}} \right] \right\}$$

SPHERICAL BASIS FUNCTIONS

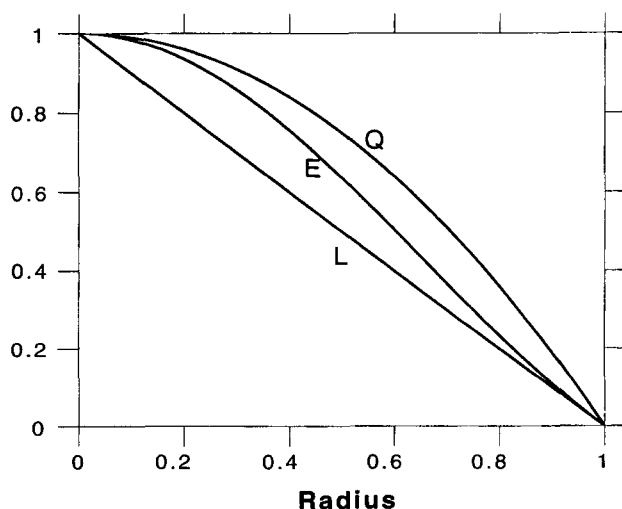


Figure 1. Comparison of linear ($L = 1 - x$) and quadratic ($Q = 1 - x^2$) basis functions with the leading eigenfunction ($E = \sin(\pi x)/\pi x$) of the diffusion equation in a sphere.

and Galerkin projection. Bearing in mind that the exact solution for this case is $K = \pi^2 = 9.870$, the Galerkin projection is seen to be superior to volume averaging, and the best approximation, $K = 10$, results with a linear spatial profile.

A linear spatial profile cannot of course satisfy the boundary condition at the center of the pellet, and on this basis one might expect the linear approximation to be poor or even inconsistent. The objective however is not to describe the dynamics near the pellet center, but rather to find the best description of the global response of the pellet. Conditions near the center make an insignificant contribution to the overall mass balance. Moreover, the boundary condition at the center has already been accounted for in the integral form expressed by Eq. 13.

The reason that the linear profile is *superior* to the quadratic may be seen by comparing the linear and quadratic profiles with the first basis function of the exact solution: $\sin(\pi x)/\pi x$. This comparison is plotted in Figure 1 where it is evident that the linear basis function is much closer to the exact basis function over most of the pellet volume. The quadratic basis does match the leading eigenfunction better near the pellet center but this region is tiny, particularly in a volumetric sense (being weighted with x^2 in the integral mass balance). As shown in Eq. 10a the concentration profile is quadratic at slow modulation because *all* Fourier modes participate in the dy-

namics, whereas only the leading eigenfunction dominates the long time response when the surface concentration is constant. Thus, there is no fundamental reason for using a quadratic or higher-order function to develop an approximate solution of the unit step response in spherical pellets.

Global approximations of this sort, however, fail to account for most of the saturation, which occurs at short times! To capture the short time response to a unit step in external concentration, a penetration theory is developed. A moving finite element is introduced over which the concentration varies either linearly

$$C(x, t) = \frac{x - \delta(t)}{1 - \delta(t)}, \quad (16a)$$

or quadratically

$$C(x, t) = \left(\frac{x - \delta(t)}{1 - \delta(t)} \right)^2, \quad (16b)$$

on the range $\delta \leq x \leq 1$, and is zero for $0 \leq x \leq \delta$. The position of the node at $x = \delta(t)$ is the free parameter in the approximation, and marks the edge of the concentration front. The loading L is related to $\delta(t)$ as:

$$L = 1 - \frac{(1 + \delta)(1 + \delta^2)}{4}, \quad (17a)$$

in the linear case, and as:

$$L = \frac{6 - 3\delta - 2\delta^2 - \delta^3}{10}, \quad (17b)$$

with the quadratic profile. When $\delta = 0$, penetration theory ends and the long time (LDF) approximations developed earlier apply. Note that the relative saturation at the start of the LDF model is 75% or 60% with linear or quadratic profiles respectively, and reflects the large weight given to the outer regions of the pellet in spherical geometry.

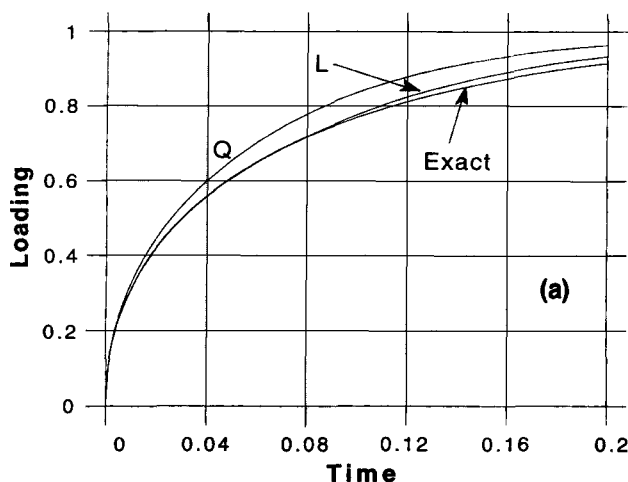
Though volume balance on the moving element is straightforward, Galerkin approximation must be interpreted more broadly as now the function is pinned at both nodes, and the free variable is the position of the edge of the boundary layer. Standard Galerkin projection corresponds to minimization of the integral square error with respect to function velocity dC/dt , and in moving finite element theory the mesh is set analogously by minimization with respect to nodal velocity $d\delta/dt$ (Miller and Miller, 1981). This yields weighting functions of $w(x) = 1 - x$ for linear approximation, and $w(x, t) = (1 - x)(x - \delta)$ for the quadratic case.

When the penetration is slight ($\delta \approx 1$) the rate equation with either volume or Galerkin projection may be reduced to the quadratic form in which Q is a constant:

$$\frac{dL}{dt} = \frac{Q}{L}, \quad (18)$$

and shows that the approximate solutions have the requisite square root singularity at $t = 0$. Values of Q derived with linear and quadratic profiles under volume averaging and Galerkin

UNIT STEP SOLUTION: VOLUME BALANCE



UNIT STEP SOLUTION: GALERKIN PROJECTION

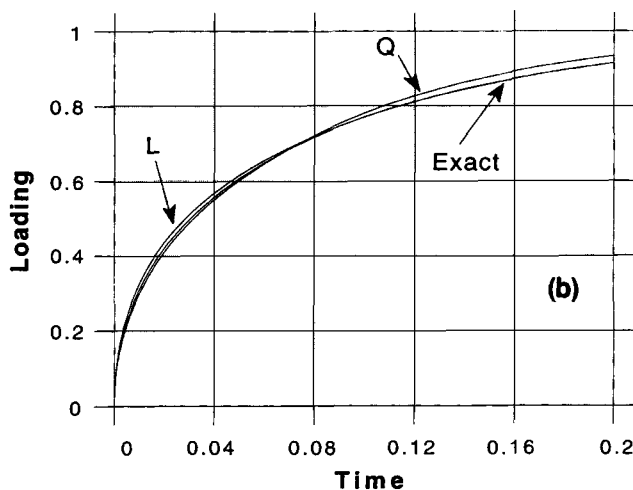


Figure 2. Finite element approximations to the unit step solution: a. volume average; b. Galerkin projection.

projection are listed in Table 2 and indicate that the asymptote of the exact solution: $Q = 18/\pi = 5.730$ is closely matched by all methods. It is not possible to derive an explicit equation for the loading over the full range of δ so the solution is presented parametrically in Table 2 as: $t = t(\delta)$, $L = L(\delta)$ where the relationship between loading L and front coordinate δ has been defined in Eq. 17.

Comparison of approximate solutions formed by joining penetration and LDF models to the exact solution of the unit step response is made in Figure 2. The fit is generally excellent. Galerkin projection is more accurate than volume balance and the linear profile is superior to the quadratic; though quadratic interpolation provides a slightly better match to the initial singularity, the error at long times is larger. Unfortunately the parametric form of the solution at small times makes these formulae inconvenient.

It is important to point out that a very convenient approximate formula for the unit step response may be constructed by blending short and long time asymptotes of the sorption

rate. Addition of the asymptotes gives the following differential equation for loading:

$$\frac{dL}{dt} = \frac{Q}{L} + K(1-L) + M(L), \quad (19)$$

in which the function M is to be determined so that the composite formula has the correct leading order asymptotic behavior (Nayfeh, 1981). At short times ($L \rightarrow 0$) the formula is dominated by the singular part, Q/L , and no correction is needed. At long times ($L \rightarrow 1$), $M(L) = -Q - Q(1-L)$ preserves the $K(1-L)$ rate of exponential decay at leading order in $(1-L)$. The simplest choice is to set $M(L) = Q(L-2)$ for all values of L so the composite rate law reads:

$$\frac{dL}{dt} = (1-L) \left(K - Q + \frac{Q}{L} \right), \quad (20)$$

which may be integrated to:

$$\ln [1-L] + \left(\frac{Q}{K-Q} \right) \ln \left[\left(\frac{K-Q}{Q} \right) L + 1 \right] = -Kt. \quad (21)$$

The quadratic mass-transfer law proposed by Glueckauf (1955) corresponds to $K=4Q$ and is difficult to justify since the exact coefficients are in the ratio of $K/Q = \pi^3/18 = 1.723$. The choice of $K=2Q$ is closer to the exact ratio and reduces the differential equation for mass transfer to the symmetric form

$$\frac{dL}{dt} = K \left(\frac{1-L^2}{2L} \right), \quad (22)$$

which is the QDF law proposed by Vermeulen (1953) if $K = \pi^2$. The spirit of simplicity is best served with round numbers for coefficients, so the choice of $K=10$ yields the following formula for loading

$$L(t) = \sqrt{1 - e^{-10t}}, \quad (23)$$

which is shown to be a close approximation to the exact solution in Figure 3a. At short times this QDF law predicts that $L = \sqrt{10t}$ (7% too low), and the mass-transfer coefficient at long times, $K=10$, is within 1% of the exact value. By contrast the standard LDF model ($K=15$) misses the sharp response at short times and overpredicts by 50% the mass-transfer rate close to equilibrium.

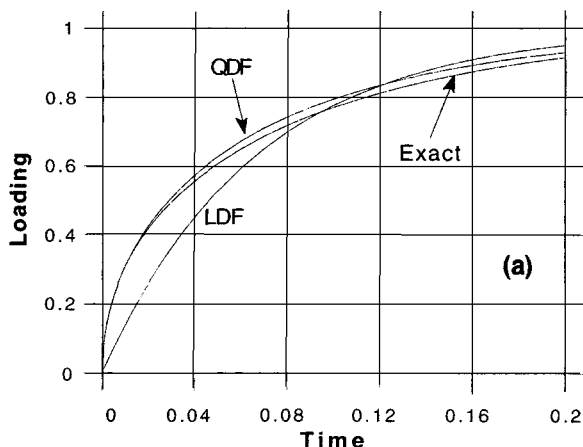
Implementation

To obtain a useful model of diffusional mass transfer for adsorption process simulation, it is necessary to generalize the unit step response to permit arbitrary concentration variation $\Gamma(t)$ at the pellet surface. For this reason the LDF model is typically applied in differential form as:

$$\frac{dL}{dt} = K(\Gamma - L), \quad (24)$$

and then integrated along with column balances such as Eq.

UNIT STEP ADSORPTION: SIMPLE APPROXIMATIONS



UNIT STEP DESORPTION: SIMPLE APPROXIMATIONS

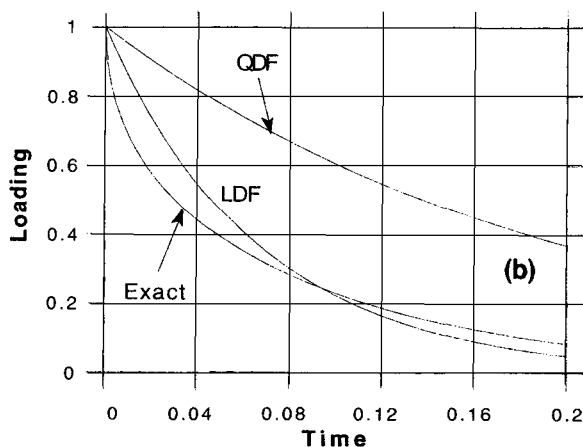


Figure 3. LDF and QDF models of the unit step solution: a. adsorption; b. desorption.

0 to obtain the solution. Although the LDF model is only valid close to saturation it describes both desorption and adsorption with comparable accuracy.

The more accurate, nonlinear formulae do not generalize as readily. The finite element solutions, though the most accurate of the simple approximations considered here, cannot be cast as a differential equation for loading. Extension of the QDF model by substitution of $\Gamma(t)$ for surface concentration yields the conventional form of the QDF law (Glueckauf, 1955):

$$\frac{dL}{dt} = K \left(\frac{\Gamma^2 - L^2}{2L} \right). \quad (25)$$

While Eq. 25 predicts adsorption ($\Gamma=1$) well, on desorption ($\Gamma=0$) it reduces to LDF form with coefficient $K/2$ and is therefore less accurate than the standard LDF model, as shown in Figure 3b. Although the QDF law is easily extended to cover desorption from a uniform pellet by recognizing that the singular response as $t \rightarrow 0$ is due to the difference between initial and boundary conditions it is not evident how L_0 should be defined in a cyclic process, as the concentration profile within the pellet changes continually in response to external condi-

tions, and is rarely uniform. All rate laws which capture the short time response of the unit step solution suffer this limitation.

The rigorous generalization of diffusional mass transfer for the linear problem must account for memory effects which are embedded in the convolution integral. Note that the unit step response Ψ could be generated by various means: from exact or approximate formulae or in cases of more general diffusion than can be accommodated by Eq. 5, by either numerical solution or experimental measurements of uptake.

Equations for the rate of uptake may be obtained by differentiation of the memory integral, Eq. 8b, with specific forms of unit step solution Ψ . If the LDF solution of the unit step response is substituted for Ψ then the differential form of the LDF law is recovered, Eq. 24. When the QDF approximation to the unit step response is used, differentiation of the memory integral does not yield the standard QDF law. The QDF law, Eq. 25, is recovered however if convolution is made with Ψ^2 instead of Ψ . This is inconsistent with the linear mathematics of the diffusion equation, and indicates that the differential form of the QDF law is not generally valid.

To apply convolution efficiently in process simulation, the range of integration is restricted to the saturation time θ :

$$L(z, t) = \Gamma(z, t - \theta) + \int_0^\theta \Psi(\zeta) \frac{\partial \Gamma}{\partial t}(z, t - \zeta) d\zeta. \quad (26)$$

In practice, $\theta = 1$ is sufficient to ensure accuracy of 10^{-4} in the loading. When the kernel is smooth, quadrature is carried out by trapezoid rule on a variable grid to meet a local error criterion (Gresho et al., 1980). At transitions between steps in process simulation, the concentration may be discontinuous and in this case the integral reduces to the unit step response, scaled with the magnitude of concentration jump.

An additional benefit of using the memory integral, Eq. 26, to calculate loading directly is that solid phase equations may be dropped, reducing the number of equations for column dynamic simulation by nearly half. With implicit integration in time the computational work scales from \mathcal{N}^2 to \mathcal{N}^3 where \mathcal{N} is the number of dynamic equations generated by spatial discretization so the simulation may run 4 to 8 times faster if the time spent evaluating the memory integral is low. This approach is being tested and will be reported on in a companion article, along with additional simplifications from asymptotic expansion of the unit step response.

Demonstration: Simple Cycles

To demonstrate the memory integral method, the response of a single pellet will be studied under conditions of known variation in external concentration. This is a rough representation of kinetic separation processes which by design limit the penetration of the slowly diffusing species in the adsorbent. Under these conditions, changes in concentration of the "slow" component made at either end of the column propagate quickly, and in the limit of high selectivity, the solid throughout the bed responds in step to the prescribed fluid concentration. Of particular interest are cyclic solutions; only these will be discussed.

The range of cycle times studied was chosen to be representative of kinetic separations. The $O(10)$ values for the LDF

coefficients presented in Table 1 indicate that the pellet saturates in $O(10^{-1})$ dimensionless time. A kinetic process must operate an order of magnitude faster than this, to restrict transport of the more slowly diffusing component. Accordingly results are presented for dimensionless periods p in the range $0.01 \leq p \leq 0.1$.

Two cases were considered. The first case corresponds to sinusoidal forcing of the pellet at period $p = 2\pi/\omega$:

$$\Gamma(t) = \frac{1 + \sin(\omega t)}{2}, \quad (27)$$

for which the exact solution is a damped harmonic with phase lag:

$$L(t) = \frac{1 + A \sin(\omega t + \phi)}{2}, \quad (28a)$$

$$A = \sqrt{a^2 + b^2}, \quad (28b)$$

$$\phi = \tan^{-1}(a/b), \quad (28c)$$

$$a = \frac{3}{4\alpha} \frac{\sinh(\alpha) \cosh(\alpha) - \sin(\alpha) \cos(\alpha)}{\sinh^2(\alpha) + \sin^2(\alpha)}, \quad (28d)$$

$$b = -\frac{3}{4\alpha} \frac{\sinh(\alpha) \cosh(\alpha) + \sin(\alpha) \cos(\alpha)}{\sinh^2(\alpha) + \sin^2(\alpha)} + \frac{3}{4\alpha^2}, \quad (28e)$$

$$\alpha = \sqrt{\omega/2}. \quad (28f)$$

Note that for fast cycles ($\omega \rightarrow \infty$), the amplitude damps asymptotically as $A \rightarrow 3/(4\sqrt{\omega})$ and the phase approaches a constant: $\phi \rightarrow -\pi/4$. When the cycles are slow ($\omega \rightarrow 0$), the asymptotic form of the solution is weakly damped,

$$A \rightarrow 1 - \frac{13}{14} \left(\frac{\omega}{15} \right)^2,$$

and nearly in phase with the external concentration: $\phi \rightarrow -\omega/15$.

The LDF equations yield an analytic solution with the proper functional form but with amplitude and phase of:

$$A_{\text{LDF}} = \frac{K}{\sqrt{K^2 + \omega^2}}, \quad (29a)$$

$$\phi_{\text{LDF}} = -\tan^{-1} \left(\frac{\omega}{K} \right). \quad (29b)$$

With fast cycles the amplitude damps inversely with frequency: $A_{\text{LDF}} \rightarrow K/\omega$, and the phase lags by $\pi/2$. When the cycle is slow the asymptotic effect of frequency is $A_{\text{LDF}} \rightarrow 1 - (1/2)(\omega/K)^2$ and $\phi_{\text{LDF}} \rightarrow -\omega/K$. The standard LDF coefficient $K = 15$ matches the first-order phase lag of the solution when the cycles are slow but fails to match the second-order damping. This result is in agreement with the frequency analysis of Jury (1967). Figure 4 shows that the standard LDF model ($K = 15$) predicts excessive damping and phase lag at dimensionless periods less than 0.1.

HARMONIC PELLETT

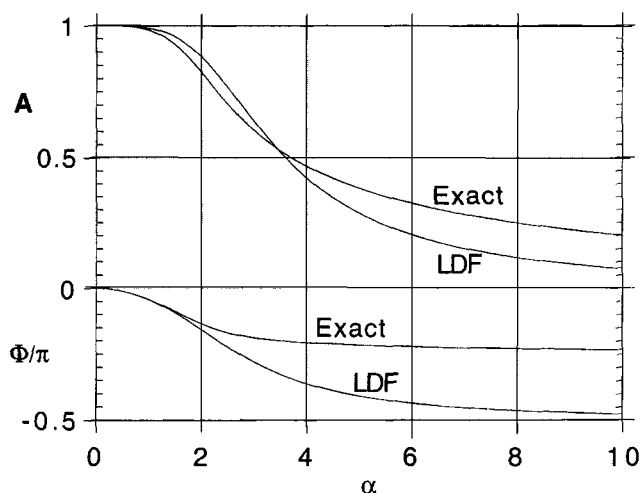


Figure 4. Amplitude and phase of the harmonic solution and the LDF approximation as a function of $\alpha = \sqrt{\omega/2}$.

The memory integral model was evaluated numerically for this cycle by trapezoid rule quadrature on a variable grid selected to meet a local error criteria of 10^{-4} . As a check of the method, the numerical results matched the analytic formula, Eq. 28, to three figures when the exact kernel was used in the memory integral. Evaluation with the QDF kernel was twice as fast and the results track the exact solution correctly in phase and amplitude, even at dimensionless periods as low as $p = 0.01$, as shown in Figure 5. The deviation from the exact solution is at most 1%, and is due to the limitations of the QDF approximation of the unit step response.

The second case considered is a square wave of dimensionless period p , in which the surface concentration of the pellet alternates between one (adsorption), and zero (desorption): $0 \leq t \leq p/2$: $\Gamma = 1$, $p/2 \leq t \leq p$: $\Gamma = 0$.

The exact solution may be derived by spatial Fourier decomposition as:

$$0 \leq t \leq p/2: L(t) = 1 - 6 \sum_{n=1}^{\infty} \frac{\alpha_n}{(n\pi)^2} e^{-(n\pi)^2 t}, \quad (30a)$$

$$p/2 \leq t \leq p: L(t) = 6 \sum_{n=1}^{\infty} \frac{\alpha_n}{(n\pi)^2} e^{-(n\pi)^2 (t-p/2)}, \quad (30b)$$

in which the Fourier coefficients are:

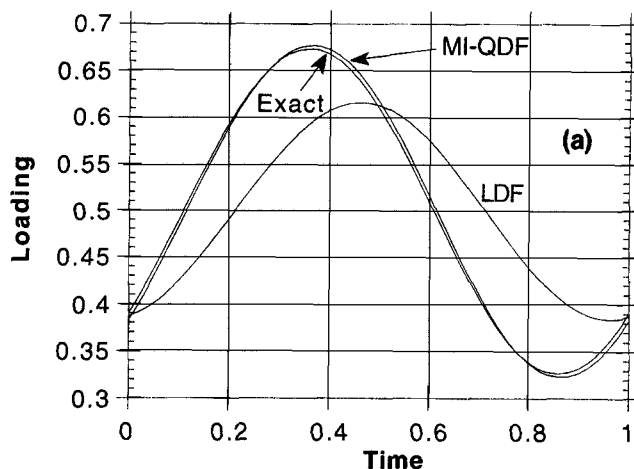
$$\alpha_n = \frac{1 - e^{-(n\pi)^2 (p/2)}}{1 - e^{-(n\pi)^2 p}}. \quad (30c)$$

The LDF model has an analytic solution of similar form as it corresponds to a single spatial mode:

$$0 \leq t \leq p/2: L_{LDF} = 1 - \Lambda e^{-Kt}, \quad (31a)$$

$$p/2 \leq t \leq p: L_{LDF} = \Lambda e^{-K(t-p/2)}, \quad (31b)$$

HARMONIC PELLETT: PERIOD = 0.1



HARMONIC PELLETT: PERIOD = 0.01

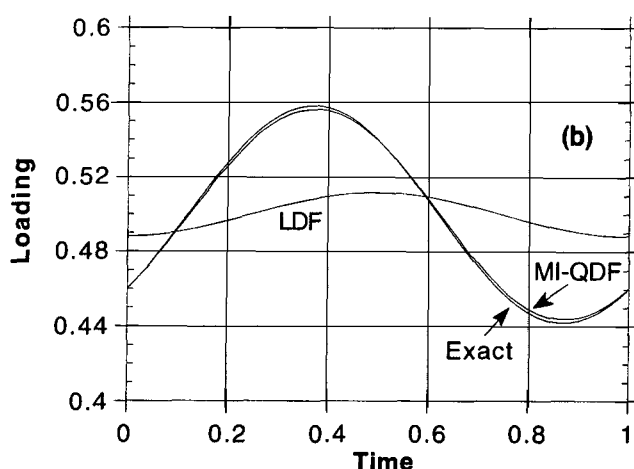


Figure 5. Concentration dynamics of the harmonic solution compared to the LDF result and the Memory-Integral model with QDF kernel: a. period = 0.1; b. period = 0.01.

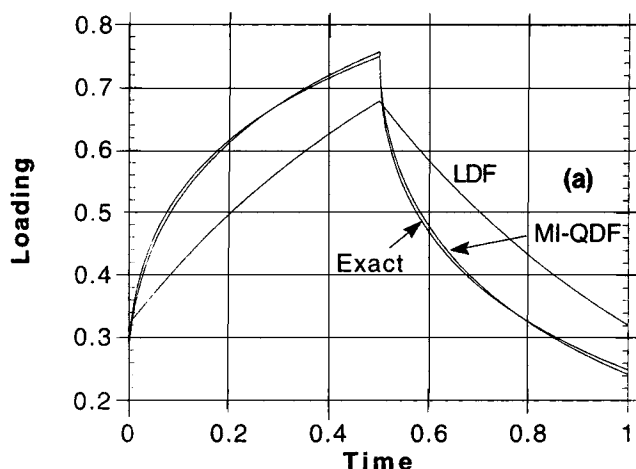
where the midpoint loading is defined as:

$$\Lambda = \frac{1 - e^{-Kp/2}}{1 - e^{-Kp}}. \quad (31c)$$

For this cycle the kernel is singular, and the integral reduces to a summation of responses to step changes in the boundary condition of the pellet. Contributions from earlier times were dropped from the sum when their contribution fell below the tolerance of 10^{-4} . As with the sinusoidal case, fast cycling required that the summation be carried out over $O(1/p)$ cycles to adequately resolve the periodic state, corresponding to a cutoff time of $\theta \approx 1$.

Comparison of the solutions is made in Figure 6. Here the phase lag is not apparent, but the excessive damping of the LDF model is. Again the memory integral model with QDF kernel matches the exact solution closely even at periods as low as 0.01. At $p = 0.1$, the deviation of the memory integral calculation from the exact solution indicates that the unit step

SQUARE WAVE CYCLE: PERIOD = 0.1



SQUARE WAVE CYCLE: PERIOD = 0.01

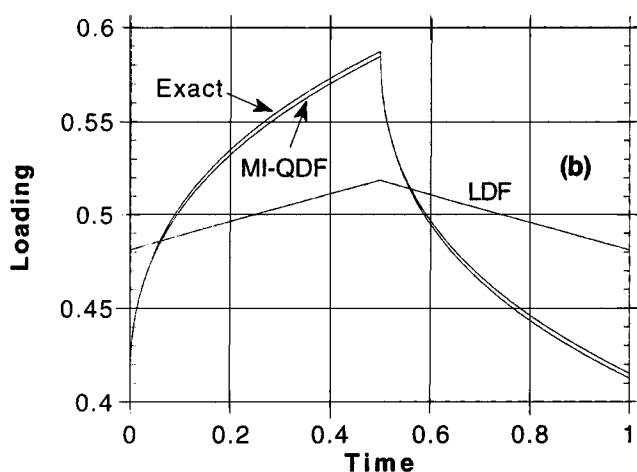


Figure 6. Concentration dynamics of a square wave cycle compared to the LDF result and the Memory-Integral model with QDF kernel: a. period = 0.1; b. period = 0.01.

response is underpredicted at short times, then overpredicted by the QDF law. At $p=0.01$, the slight error at short times is apparent, and the memory integral results lags the exact solution throughout the cycle. The error is due to the fit of the unit step response by the QDF formula, and is at most 1%.

Conclusions

Central to this article is the idea that rate laws are redundant in computational simulation of adsorption process dynamics. There is no need to involve the pellet directly in simulation of the process because the dynamics of the pellet may be computed explicitly, once the surface concentration is known. Successful implementation of this method requires that the memory integral be computed efficiently, but offers great savings as the number of equations are cut by half once the equations for the solid phase are dropped. The details of numerical computation only have been sketched here and will be presented in full by a subsequent article.

The use of the memory integral is shown to be consistent with the familiar LDF rate law when the process dynamics change slowly on the timescale for pellet saturation. The concentration profile proceeds in even powers of radius, and the leading coefficient of the asymptotic expansion for loading is $K=15$.

Approximations of the unit step response which sits within the memory integral have been reviewed and extended to short contact times. Standard concentration profiles of fixed form which span the pellet lead to an LDF model. Derivation of the LDF coefficient K was shown to depend upon the spatial profile, and the projection method used. Surprisingly the best value of K for the unit step response was obtained with a linear profile, due to the close fit with the leading eigenfunction of the exact solution near the outer surface of the pellet. This is significant as most of the efforts to improve the LDF model of the unit step response have used higher powers in radius. Here the exact LDF coefficient is π^2 rather than 15, since unlike the case of slow modulation where all modes contribute to the response, only the leading mode survives at long times when the surface concentration is constant.

The major deficiency of the LDF model of the unit step response appears at short times during which 60–75% of the pellet is saturated. This aspect of the solution was approximated parametrically by a single moving finite element. The finite element solutions fit the exact result so closely that the curves are difficult to distinguish from the exact loading when plotted over the range: $0 \leq L \leq 1$. A simpler set of only slightly less accurate approximations was developed by blending asymptotic results at short and long times. The QDF model is of this class. This establishes the connection between QDF and the diffusion equation, which had not previously been made clear.

The finite element and QDF models are superior to the LDF approximation of the unit step response at short times because they account for the difference between the initial condition of the pellet and the boundary condition at the pellet surface. Recognizing this, it is difficult to visualize how a simple differential law will properly generalize to a complex cycle where the “initial condition” of the pellet cannot be defined. Rather, it seems preferable to account for arbitrary initial conditions by convolution or memory integral. Results presented in this article demonstrate that the memory integral accurately tracks the solution at short cycle times characteristic of kinetic separations for both smooth and sharp changes in boundary conditions, without modification. The unit step response was approximated by the QDF solution, but any convenient form of the unit step response will do; for example, a numerical solution or experimental data may be used directly in the column simulation, if available.

Nonlinear sorption also plays a role in mass-transfer dynamics. Standard “nonlinearization” of mass-transfer models involves substitution of nonlinear equilibrium in the solution derived from linear theory. For the memory integral nonlinearization leads to:

$$L(z, t) = E(z, t - \theta) + \int_0^\theta \Psi(\zeta) \frac{\partial E}{\partial t}(z, t - \zeta) d\zeta. \quad (32)$$

By this manner the equilibrium capacity is correctly accounted for, but the effect of nonlinearity on the dynamics is not.

To illustrate nonlinear dynamics a bilinear isotherm is considered:

$$S(C) = \begin{cases} HC: 0 \leq C \leq 1/H \\ 1: 1/H \leq C < \infty \end{cases}, \quad (33)$$

in the "irreversible" limit of $H \gg 1$. Additionally it is assumed that the gas capacity is negligible. Adsorption dynamics may then be described by a quasi-steady balance in which diffusion in the gas phase drives an advancing front (Do, 1989) and the pellet saturates in finite time: $t \sim O(1)$. This approximate solution neglects a region ahead of the main front in which the concentration is $O(1/H)$, but describes the saturation well for $H \gg 1$. The time for saturation may be obtained from scaling arguments since the diffusive flux is driven by an $O(1)$ gradient of concentration. On desorption however, the pellet does not unload until concentration drops below $1/H$, and since the driving force for diffusion is then $O(1/H)$, a time of $O(1/H)$ is required to clean out the pellet. The ratio of the timescales for adsorption and desorption is simply the isotherm slope at low concentration: H . In a dynamic sense the label of "irreversible" is apt: even though the thermodynamics are fully reversible, the timescale for achieving equilibrium is ponderously slow for desorption and will give rise to apparent irreversibility when H is large. Numerical calculations of desorption under nonlinear equilibrium (Do, 1990) confirm the scaling law expressed above.

Dynamic asymmetry of this sort is well known in column dynamics where favorable (convex) equilibria cause concentration waves in a column to accelerate and steepen on adsorption and to spread and slow on desorption (Aris and Amundson, 1973). The effect on process performance is to accumulate a heel of unpurged material in the bed at cyclic steady state. In a pellet, nonlinear dynamics will act similarly to raise the time-averaged concentration in the pellet, and thereby reduce the working capacity of the material. Accurate modeling of these nonlinear effects within the framework of the memory integral will require a modified superposition principle to account for the slower dynamics and correspondingly longer "memory" of desorption.

Notation

C = intrapellet gas phase concentration
 D_e = effective intrapellet diffusivity
 D_c = intrapellet gas phase diffusivity
 D_s = intrapellet adsorbed phase diffusivity
 E = equilibrium solid loading
 H = linear isotherm slope (Henry's law constant)
 K = long-time mass-transfer coefficient
 L = solid loading
 N = total intrapellet concentration
 p = period of process cycle
 Q = short-time mass-transfer coefficient
 R = pellet radius
 S = intrapellet adsorbed phase concentration
 t = time
 v = superficial gas velocity
 w = finite element weighting function
 x = radial pellet coordinate
 z = axial column coordinate

Greek letters

δ = concentration front position

ϵ = interpellet void fraction
 ϕ = phase of harmonic solution
 Φ = finite element basis function
 Γ = interpellet gas concentration
 θ = saturation time
 ν = intrapellet void fraction
 ω = frequency of harmonic process cycle: $2\pi/p$
 Ψ = unit step response

Subscripts

$_0$ = initial condition

Superscript

* = scale or characteristic value

Literature Cited

- Aris, R., and N. Amundson, *Mathematical Methods in Chemical Engineering: 2. First-Order Partial Differential Equations, With Applications*, Prentice Hall, Englewood Cliffs, NJ (1973).
 Bunke, G., and D. Gelbin, "Effects of Cyclic Operation on Adsorber Performance," *Chem. Eng. Sci.*, **30**, 1301 (1975).
 Bunke, G., and D. Gelbin, "Breakthrough Curves in the Cyclic Steady State for Adsorption Systems with Concave Isotherms," *Chem. Eng. Sci.*, **33**, 101 (1978).
 Buzanowski, M. A., and R. T. Yang, "Extended Linear Driving-Force Approximation for Intraparticle Diffusion Rate Including Short Times," *Chem. Eng. Sci.*, **44**, 2683 (1989).
 Carslaw, H. S., and J. C. Jaeger, *Conduction of Heat in Solids*, Clarendon Press, Oxford, U.K. (1959).
 Do, D. D., "Sorption Rate of Bimodal Microporous Solids with an Irreversible Isotherm," *Chem. Eng. Sci.*, **44**, 1707 (1989).
 Do, D. D., "Hierarchy of Rate Models for Adsorption and Desorption in Bimodal Structured Sorbents," *Chem. Eng. Sci.*, **45**, 1373 (1990).
 Do, D. D., and P. L. J. Mayfield, "A New Simplified Model for Adsorption in a Single Particle," *AIChE J.*, **33**, 1397 (1987).
 Do, D. D., and R. G. Rice, "Validity of the Parabolic Profile Assumption in Adsorption Studies," *AIChE J.*, **32**, 149 (1986).
 Doong, S. J., and R. T. Yang, "Bidisperse Pore Diffusion Model for Zeolite Pressure Swing Adsorption," *AIChE J.*, **33**, 1045 (1987).
 Glueckauf, E., "Theory of Chromatography: 10 Formulae for Diffusion Into Spheres and Their Application to Chromatography," *Trans. Farad. Soc.*, **51**, 1540 (1955).
 Glueckauf, E., and J. I. Coates, "Theory of Chromatography: V. The Influence of Incomplete Equilibrium on the Front Boundary of Chromatograms and the Effectiveness of Separation," *J. Chem. Soc.*, 1315 (1947).
 Gorius, A., M. Bailly, and D. Tondeur, "Perturbative Solutions for Non-linear Fixed-bed Adsorption: I. Approximate Analytical Solutions for Asymptotic Fronts," *Chem. Eng. Sci.*, **46**, 677 (1991).
 Gresho, P. M., R. L. Lee, and R. L. Sani, "On the Time-Dependent Solution of the Incompressible Navier-Stokes Equations in Two and Three Dimensions," *Recent Advances in Numerical Methods in Fluids*, Vol. 1, C. Taylor and K. Morgan, eds., Pineridge Press, Swansea, U.K. (1980).
 Jury, S. H., "An Improved Version of the Rate Equation for Molecular Diffusion in a Dispersed Phase," *AIChE J.*, **13**, 1124 (1967).
 Kim, D. H., "Linear Driving Force Formulas For Diffusion and Reaction in Porous Catalysts," *AIChE J.*, **35**, 343 (1989).
 Kocirik, M., G. Tschirch, P. Struve, and M. Bulow, "Application of the Volterra Integral Equation to the Mathematical Modeling of Adsorption Kinetics under Constant-Volume/Variable-Concentration Conditions," *J. Chem. Soc., Farad. Trans. 1*, **84**, 2247 (1988).
 Liaw, C. H., J. S. P. Wang, R. A. Greenkorn, and K. C. Chao, "Kinetics of Fixed Bed Sorption: a New Solution," *AIChE J.*, **25**, 376 (1979).
 Miller, K., and R. N. Miller, "Moving Finite Elements: I," *SIAM J. Num. Anal.*, **18**, 1019 (1981).
 Nakao, S., and M. Suzuki, "Mass Transfer Coefficient in Cyclic Adsorption and Desorption," *J. Chem. Eng. Japan*, **16**, 114 (1983).

- Nayfeh, A. H., *Introduction to Perturbation Techniques*, Wiley, New York (1981).
- Oran, E. S., and J. P. Boris, *Numerical Simulation of Reactive Flow*, Elsevier, New York (1987).
- Raghavan, N. S., M. M. Hassan, and D. M. Ruthven, "Numerical Simulation of a PSA System Using a Pore Diffusion Model," *Chem. Eng. Sci.*, **41**, 2787 (1986).
- Rosen, J. B., "Kinetics of a Fixed Bed System for Solid Diffusion into Spherical Particles," *J. Chem. Phys.*, **20**, 387 (1952).
- Strang, G., and G. J. Fix, *An Analysis of the Finite Element Method*, Prentice-Hall, Englewood Cliffs, NJ (1973).
- Tomida, T., and B. J. McCoy, "Polynomial Profile Approximation for Intraparticle Diffusion," *AIChE J.*, **33**, 1908 (1987).
- Vermeulen, T., "Theory for Irreversible and Constant-Pattern Solid Diffusion," *Ind. Eng. Chem.*, **45**, 1664 (1953).

Manuscript received Apr. 20, 1992, and revision received Aug. 31, 1992.
